

SECOND-STAGE ACCELERATION IN A LIMB-OCCULTED FLARE

H. S. HUDSON

Center for Astrophysics and Space Science, UCSD

R. P. LIN

Space Science Laboratory, UCB

and

R. T. STEWART

Division of Radiophysics, CSIRO

(Received 4 August, 1980; in revised form 5 March, 1981)

Abstract. We analyze hard and soft X-ray, microwave and meter wave radio, interplanetary particle, and optical data for the complex energetic solar event of 22 July 1972. The flare responsible for the observed phenomena most likely occurred $\sim 20^\circ$ beyond the NW limb of the Sun, corresponding to an occultation height of 45 000 km. A group of type III radio bursts at meter wavelengths appeared to mark the impulsive phase of the flare, but no impulsive hard X-ray or microwave burst was observed. These impulsive-phase phenomena were apparently occulted by the solar disk as was the soft X-ray source that invariably accompanies an $H\alpha$ flare. Nevertheless essentially all of the characteristic phenomena associated with second-stage acceleration in flares – type II radio burst, gradual second stage hard X-ray burst, meter wave flare continuum (FC II), extended microwave continuum, energetic electrons and ions in the interplanetary medium – were observed. The spectrum of the escaping electrons observed near Earth was approximately the same as that of the solar population and extended to well above 1 MeV.

Our analysis of the data leads to the following results: (1) All characteristics are consistent with a hard X-ray source density $n_i \sim 10^8 \text{ cm}^{-3}$ and magnetic field strength ~ 10 G. (2) The second-stage acceleration was a physically distinct phenomenon which occurred for tens of minutes following the impulsive phase. (3) The acceleration occurred continuously throughout the event and was spatially widespread. (4) The accelerating agent was very likely the shock wave associated with the type II burst. (5) The emission mechanism for the meter-wave flare continuum source may have been plasma-wave conversion, rather than gyrosynchrotron emission.

1. Introduction

It has long been known from radio observations that two distinct groups of phenomena occur in large solar flares (Wild *et al.*, 1963): an impulsive phase of $\sim 10^2$ s duration in the early stage of a flare, characterized by an impulsive microwave burst and type III radio bursts; and a following second phase lasting for tens of minutes and characterized by type II and type IV bursts and by microwave and meter-wave continuum. These radio observations and later spacecraft observations of energetic particles, hard X-rays and gamma-rays indicated that the two phases correspond to two distinct episodes of particle acceleration (see Lin, 1974, for review). Gradual bursts of hard X-rays lasting for tens of minutes were discovered to be characteristic of the flare second stage, as were coronal transients, interplanetary shocks, and long-lived soft X-ray flare loops. Interplanetary particle

measurements have shown that while $10\text{--}10^2$ keV electrons are commonly accelerated in the impulsive phase, relativistic electrons and >10 MeV protons are only accelerated in flares that exhibit a second stage. In large flares on the disk it is difficult to separate the impulsive and second stage phenomena; often the two phases are intermixed. Recently Hudson (1978) reported the observation of a gradual second stage hard X-ray burst which was associated with a limb-occulted flare event, indicating an origin relatively high in the corona. Such events provide the most unambiguous information on second stage particle acceleration because of the spatial isolation of the coronal phenomena made possible by the limb occultation.

We present here a study of the limb-occulted flare event of 22 July 1972, for which especially comprehensive observations exist. In contrast to other studies of coronal transient phenomena (Dulk *et al.*, 1976; Gergely *et al.*, 1979; Stewart *et al.*, 1974a, b) this paper concentrates on the second stage particle acceleration; thus we emphasize the hard X-ray, energetic particle and radio observations. Our analysis shows that second stage acceleration is physically distinct from the impulsive phase, and is characterized by continuous and widespread electron acceleration to high energies, most likely by the type II burst shock wave.

2. Observations

A. RADIO

The radio observations from the Culgoora radioheliograph and dynamic spectrograph provide a convenient framework for the discussion of the 22 July 1972 solar event. Figure 1 shows the dynamic spectrum and Figure 2 the locations of the meter-wavelength emissions. Groups of type III bursts at $\sim 03:31$ and $\sim 03:40$ UT appear to define the impulsive phase. The second stage begins with type II burst onset at $\sim 03:40$ UT.

From the frequency drift of the main components in the type II burst we derive a height-time plot (Figure 3) for the shock disturbance by converting fundamental or second-harmonic frequencies to height using a standard coronal density model (Newkirk, 1961). Most of the type II components from 03:40 UT fit a single-line plot which extrapolates back to the photosphere at the time of the first group of type III bursts ($\sim 03:31$ UT), which we take to identify the impulsive start of the flare. The plot gives a radial velocity component ~ 630 km s $^{-1}$ for the shock wave disturbance.

The exciter reached 80 MHz at about 03:41 UT, near the starting time of a flare continuum event of type FC II this suggests that the flare continuum (FC) was initiated by the passage of the shock wave through this part of the corona. We adopt the interpretation of Robinson and Smerd (1975) that the FC is caused by energetic electrons accelerated locally in the source region by the passage of the shock wave.

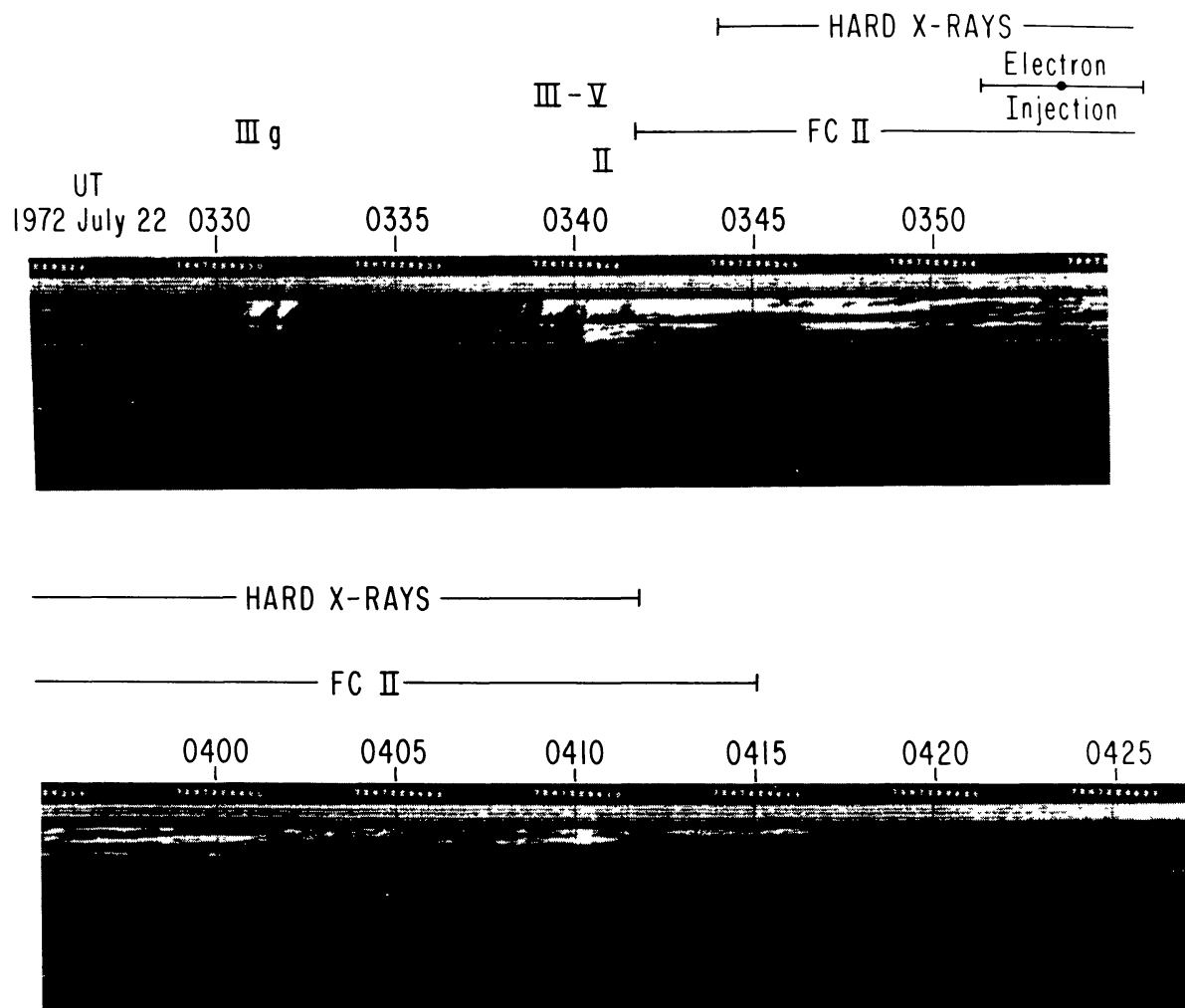


Fig. 1. Dynamic spectrum (Culgoora) of the meter-wave sources, showing the time duration of the X-ray burst observed by OSO-7. The dynamic spectrum, covering the meter-decimeter wavelengths, shows bursts of type III, type II, type V, and flare continuum (FC II). The plot also indicates the computed time of electron injection (see text).

The type II and FC sources were both located above the northwest portion of the disk. An eruptive $H\alpha$ prominence positioned over the northwest limb below the radio burst locations (see Figure 2) became activated at the time of the flare. Thus the radio and optical observations indicate that a flare occurred not too far beyond the west limb.

In addition a weak microwave and decimeter continuum burst was observed by radiometers at Hiraio and Toyokawa, Japan (*NOAA Solar-Geophysical Data*). There were no position observations for this event but it seems most likely that it too occurred above the west limb of the Sun. This gradual event lasted from 03:42 to 04:12 UT and reached maximum intensity at $\sim 03:50$ UT. From the time profile, it appears to be closely associated with the gradual hard X-ray burst (see later discussion).

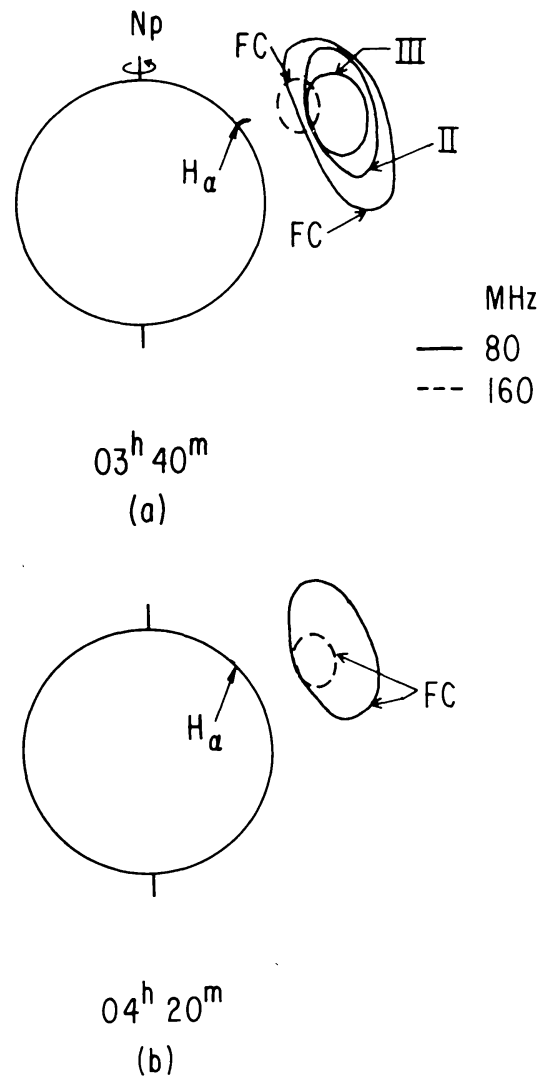


Fig. 2. Sketch of locations of the radio sources above the NW limb at (a) 03:50 UT and (b) 04:20 UT, observed at 80 MHz and 160 MHz from Culgoora. $H\alpha$ prominence observations ($H\alpha \pm 3 \text{ \AA}$) obtained by the Culgoora limb patrol telescope are also shown.

The combined spectrum of the FC and microwave continuum bursts at $\sim 03:50$ UT is plotted in Figure 4. Note that the V-shaped spectrum clearly shows the two components, *viz.* the FC events at frequencies < 200 MHz and the microwave event at frequencies > 200 MHz. The latter has a maximum at ~ 1 GHz. The microwave spectrum above 1 GHz can be interpreted as optically-thin gyroresonance emission, from particles of energies determined by the magnetic field intensity in the source. For fields on the order of 10 G, the microwave spectrum in the 1–10 GHz range is emitted by electrons in the energy range 3–10 MeV. Although this estimate is very uncertain, it at least indicates that the microwave-emitting electrons have considerably higher energies than those responsible for the 5–200 keV bremsstrahlung X-rays discussed below. We may make the standard assumption that the high-frequency part of the microwave spectrum does not suffer from self-absorption.

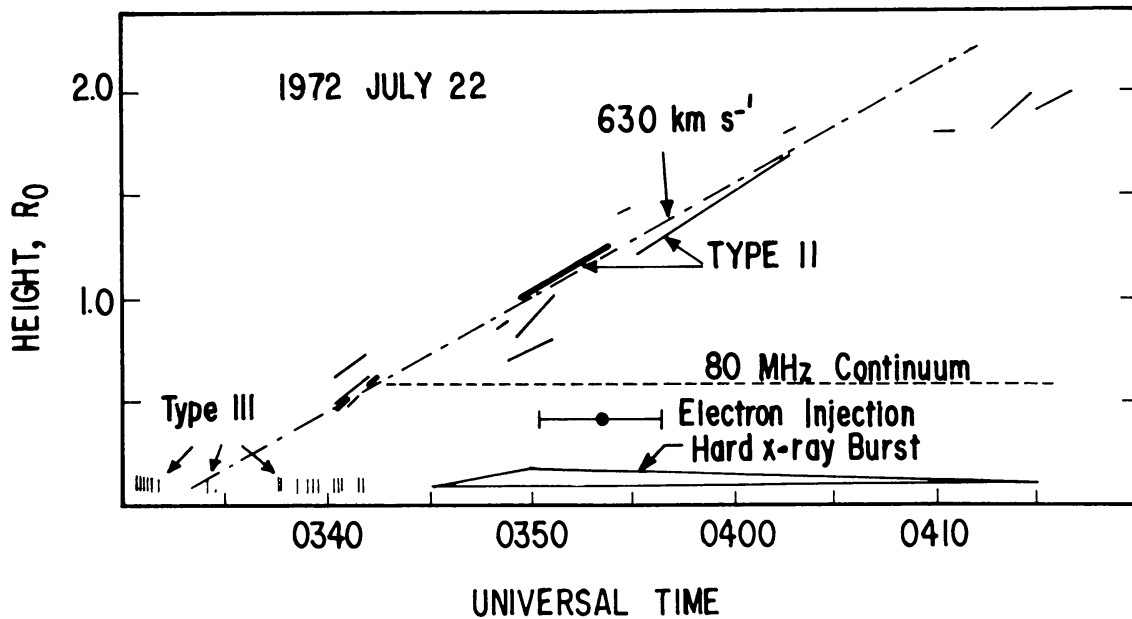


Fig. 3. Height-time plot of the type II burst of 22 June 1972. Heavy sloping lines indicate (assumed fundamental) type II bands, medium sloping lines represent (assumed second harmonic) bands. The light broken line indicates a shock speed $\sim 630 \text{ km s}^{-1}$. Type II frequencies were converted to heights using the Newkirk (1961) coronal streamer density model. Also shown on are the times of type III bursts (vertical bars), the flare continuum source at 80 MHz at an observed height $\sim 0.6 R_{\odot}$, and the time profile of the hard X-ray burst. Error bar indicates the injection time inferred from interplanetary observations (see below).

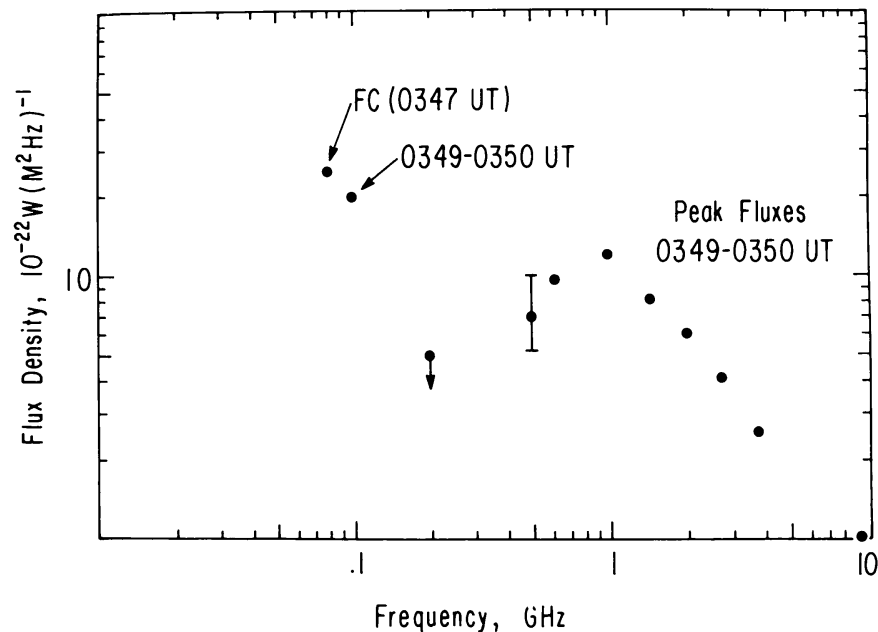


Fig. 4. Radio spectrum of event maximum, showing the microwave maximum at $\sim 1 \text{ GHz}$ and the bright m -wave source. Radio fluxes (Toyokawa and Hiraïso) were obtained from *Solar Geophysical Data*.

Then the slope α of the radio spectrum $f_\nu \sim \nu^{-\alpha}$ determines the power-law index δ of the electron distribution, $\delta = 2\alpha + 1$ in the relativistic limit (e.g., Tucker, 1975). Thus for $\alpha \sim 1$ we find $\delta \sim 3$ in the ~ 3 –10 MeV range.

B. X-RADIATION

Figure 5 shows the counting rates of hard (21.2–32.0 keV) X-rays detected by the OSO-7 solar X-ray instrument. These show a gradual hard X-ray burst strongly resembling that described by Hudson (1978) for the event of December 14 1971. Within limits of counting statistics, no rapid fluctuations occurred. The soft X-ray burst normally expected to accompany a major energetic solar event was not detected, and the soft X-ray variations detected by OSO-7 are fully explicable by the normal variations in integrated solar flux caused mainly by the active regions on the visible hemisphere. The onset of the hard X-ray event lagged significantly ~ 5 min) behind the appearance of the type II burst and the 80 MHz continuum.

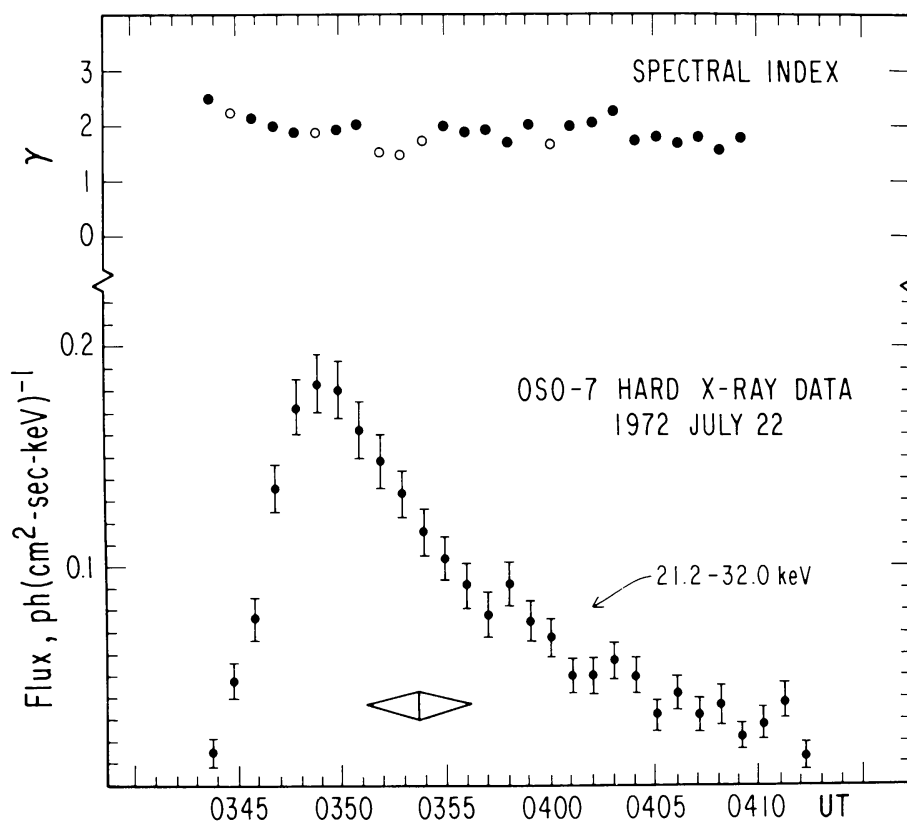


Fig. 5. OSO-7 X-ray counting rate in a representative hard (21.2–32 keV) X-ray energy channel. Background has been subtracted. The spectral index γ is also plotted, with filled circles indicating single-power-law fits from the Elcan (1979) fitting procedure. Open circles are the low-energy slopes in cases requiring a double power-law fit. The constancy of the spectrum during the event is indicated by the lack of variation of the spectral index; errors in the determination may be judged from the scatter of the points. The double triangle indicates the time ($\pm 1\sigma$) of electron injection.

The hard X-ray spectrum (Figure 6) was extremely flat; spectral fits in the 5–200 keV energy range closely match a number spectral index γ of 2.0. A spectrum-fitting algorithm (Elcan, 1979) applied to each individual one-minute

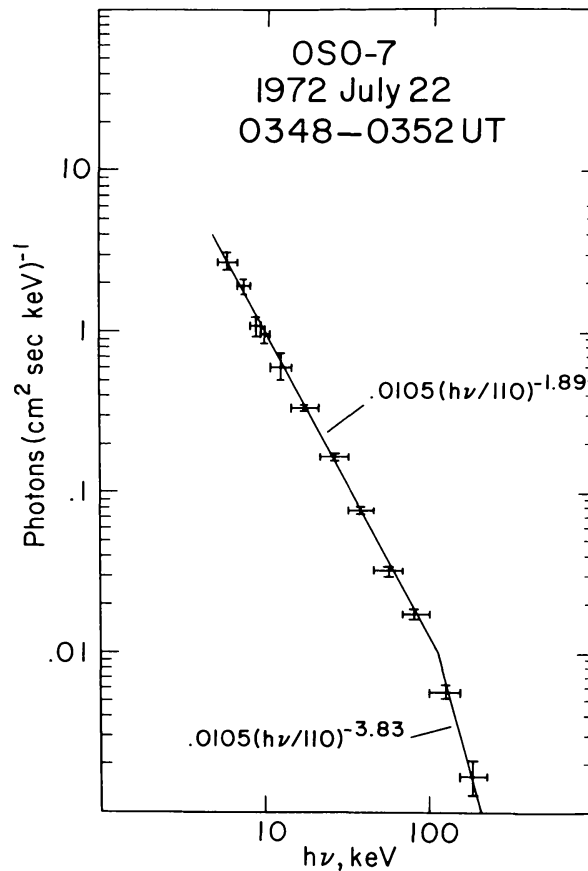


Fig. 6. X-ray spectrum from OSO-7 near event maximum (03:48-03:52 UT) showing an extremely flat spectrum over the range 5.1-229 keV. The double power-law fit shown steepens from an index 1.89 to 3.83 at 110 keV; the fit has $\chi^2 = 1.84$ per degree of freedom.

integration generally found a consistent single-power-law fit over the entire spectral range, although occasional spectra suggested a downward break (~ 0.5 in the power-law index) at energies ~ 100 keV. The point-by-point values of γ are plotted in Figure 5, and show no statistically significant deviation from the E^{-2} spectral form after 03:47 UT. The spectrum at the event onset (before 03:47 UT) was slightly softer ($\gamma \sim 2.5$). A similar early spectral steepness was observed in the 14 December 1971 event (Hudson, 1978).

The smooth time profile and lack of spectral variability from 03:47 UT to the end of the burst imply a continuous injection of fast electrons into the X-ray source. Impulsive injection followed by collisional energy loss or any energy-dependent loss or escape mechanism would result in systematic variation of the spectrum, which was not observed, during the evolution of the burst.

The near-simultaneity of the meter-wave FC source, the microwave-decimeter event and the hard X-ray event suggests a common origin in a single population of non-thermal electrons. From the X-ray spectrum we can derive the instantaneous spectrum of the electrons in the X-ray source. From the photon spectrum at burst maximum,

$$\Phi_{h\nu} = 0.25 (h\nu/20 \text{ keV})^{-2} \text{ ph (cm}^2 \text{ s keV)}^{-1}, \quad (1)$$

we obtain

$$\frac{dN}{dE} = 9.1 \times 10^{43} n_i^{-1} E^{-1.5} \text{ keV}^{-1}, \quad (2)$$

where $h\nu$ and E are the photon and electron energy respectively; n_i the average ion density and dN/dE the total number of electrons (per keV) in the source at that instant. Note here that the X-ray observations indicate a power-law exponent of ~ 1.5 in the $10\text{--}10^2$ keV region compared to ~ 3 in the few MeV region from microwave measurements. Thus there must be a downward break in the spectrum at E_b for which $100 \text{ keV} < E_b < 3 \text{ MeV}$. The spectrum in Figure 6 suggests the existence of a break in the X-ray spectrum at 110 keV.

A lower limit to the total number of electrons injected into the X-ray source over the entire event can be obtained using the thick target approximation, i.e., by assuming only Coulomb collision losses are important. The rate of injection is

$$\frac{d^2N}{dE dt} = 5.2 \times 10^{35} E^{-3} \text{ electrons (keV s)}^{-1} \quad (3)$$

Integrated over energy and event duration of ~ 500 s (FWHM), the minimum total number of electrons was $\sim 3.2 \times 10^{35}$ above 20 keV.

C. INTERPLANETARY PARTICLES

Energetic electrons were observed by the IMP-6 spacecraft to arrive at Earth orbit shortly after the onset of the radio and X-ray event (Figure 7). The electron fluxes rose rapidly after onset and then decayed slowly in a profile typical of events from flares in the W 20–W 80 fast propagation region. Velocity dispersion was observed, with the highest energy electrons arriving first as expected. The slow decay indicates

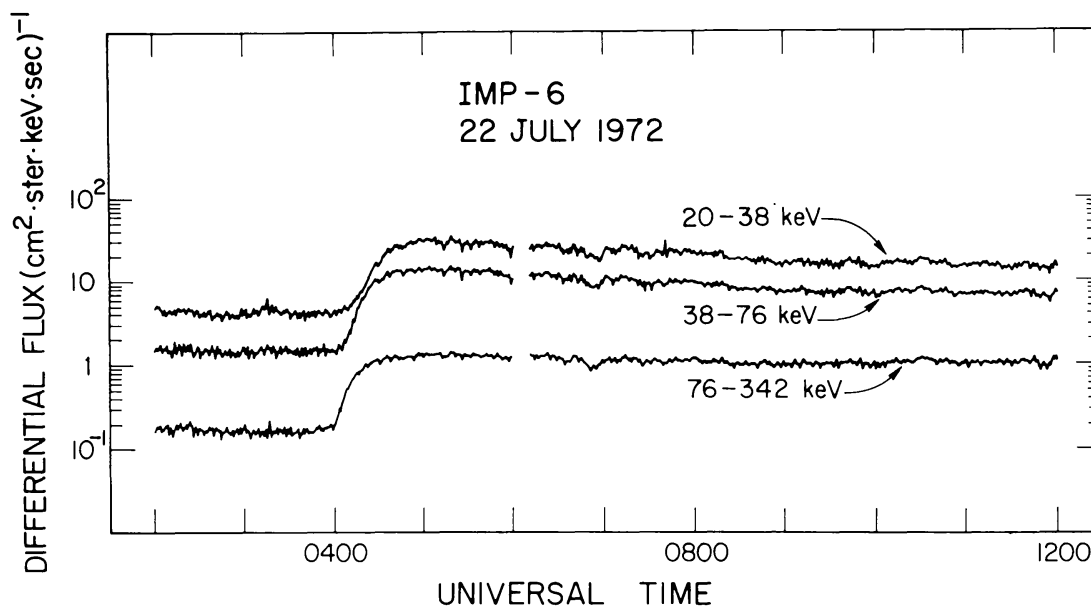


Fig. 7. Time profile of electrons recorded by IMP-6. The impulsive onset is typical of events in the 'fast propagation zone', normally W 20–W 80.

that scattering of the electrons occurs in the interplanetary medium, i.e., the particles effectively diffuse through the interplanetary medium.

Energetic protons (van Hollebeke *et al.*, 1975) were also observed from this flare. At lower energies the proton event showed a complex time profile, with a fast rise and decay (total duration > one day) superposed on a much slower event lasting for many days. Van Hollebeke *et al.* attribute the slower event to the active region, then at W 180, that later produced the 1972 August flares. The rapid proton event appears to have been associated with the same near-the-limb flare that produced the X-ray, radio, and electron phenomena presented here.

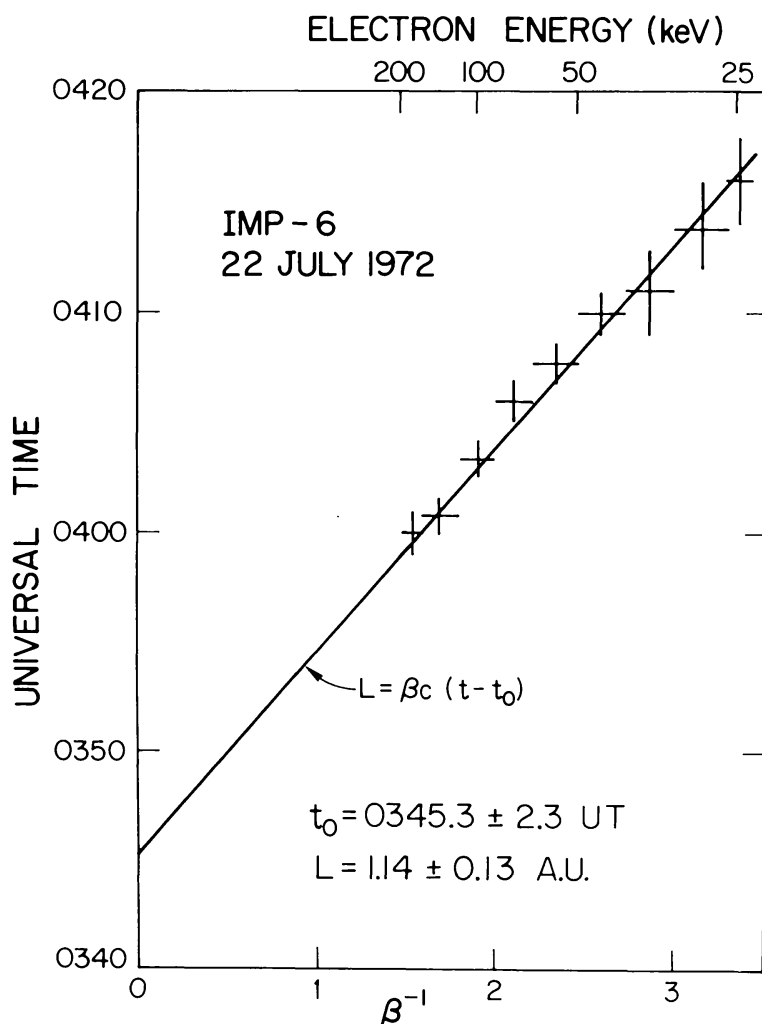


Fig. 8. Time-of-flight graph for the 25–200 keV electrons observed by IMP-6, obtained by plotting onset time versus travel time ($\sim 1/\beta$) for different energy bands. The zero intercept is taken as the injection time, the path travelled is a typical spiral field-line length.

We have analyzed the electron velocity dispersion to obtain the injection time, t_0 , as shown in Figure 8. The first-arriving electrons are those which have undergone little or no scattering. If electrons at all energies are released from the sun simultaneously at t_0 and then travel along the same length L of the spiral interplanetary

magnetic-field line to reach Earth's orbit, the onset time $t(\beta)$ for each velocity $\beta = v/c$ should be determined by

$$L = \beta c [t(\beta) - t_0]. \quad (4)$$

The plot in Figure 8 of $1/\beta$ against $t(\beta)$ shows a good fit to a straight line, indicating consistency with the assumptions. The inferred value of $L = 1.14 \pm 0.13$ is equal to the computed length for a smooth spiral interplanetary field line from the Sun to Earth orbit, based on the observed solar wind velocity of $383 \text{ km}^{-1} \text{ s}$ (Pioneer 6 measurements from *Solar Geophysical Data*). The small value of L is consistent with the rapid rise observed for the event; the implication is that particles were injected near the foot of the field lines connected to the Earth (W 60 solar longitude), and that little or no coronal diffusion across the solar disk occurred. Electron events from flares in the eastern solar hemisphere, for which substantial coronal diffusion occurs, typically show slow rises and values of L substantially greater than the smooth spiral field line length. Thus the energetic electrons observed at Earth orbit from this event appeared to be accelerated and injected into the interplanetary medium right at the footpoint of the field line at W 60 longitude.

The injection time of $03:45.3 \pm 2.3$ ($03:53.6 \pm 2.3$ corrected for light travel time to the Earth) is significantly *delayed* relative to the impulsive phase (by ~ 22 min), to the FC onset (by ~ 10 min), and to the X-ray peak time (by ~ 5 min). We interpret this late injection onto a field line remote from the flare site as evidence that the acceleration agent required this time to travel from the flare to the injection longitude of W 60. A 50° separation implies a speed of $\sim 600 \text{ km s}^{-1}$ at a height of $0.4 R_\odot$ to reach W 60, roughly consistent with the measured speed of the type II exciter $\sim 630 \text{ km s}^{-1}$.

The spectrum of the electrons at maximum flux in each energy interval is shown in Figure 9. For diffusive events the energy spectrum obtained in this manner reflects the spectrum of the particles injected at the Sun, provided only that the effective diffusion coefficient for these particles shows the same radial dependence at all energies. The numerical value of the diffusion coefficient may vary with energy without affecting this relationship between injected and observed spectra (Lin *et al.*, 1981). We have checked and found that the radial variation is in fact the same over this energy range, so that Figure 9 does give the shape of the injection spectrum. We note that it shows the typical behavior for electrons in large energetic proton events which are produced by second-stage acceleration, namely a break in the power law to a much steeper power law spectrum above ~ 100 – 200 keV (Lin *et al.*, 1981). Below $\sim 100 \text{ keV}$ the electron flux spectrum fits a power law with exponent 1.7, steepening gradually to 3.7 above $\sim 200 \text{ keV}$.

The total number of electrons injected into the interplanetary medium can be estimated given the angular extent of the cone of interplanetary field lines filled with particles. Based on the apparent location of the flare this cone must have been $\sim 60^\circ$. The total volume filled with electrons would then be $V \sim 10^{40} \text{ cm}^3$ for a depth of 2 AU. The density of fast electrons (velocity v) at maximum is given in

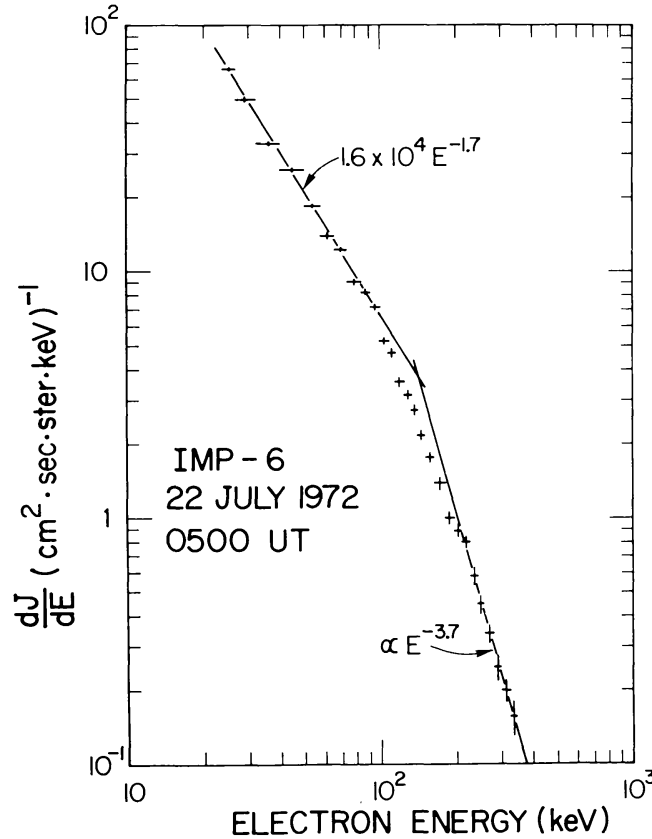


Fig. 9. Spectrum of interplanetary electrons. The two lines give high-energy and low-energy asymptotic power laws; typically the high-energy power law extends to several MeV (Lin *et al.*, 1981).

terms of the differential flux dJ/dE (particles $\text{cm}^{-2} \text{s}^{-1} \text{keV}^{-1} \text{sr}^{-1}$):

$$\begin{aligned} \frac{dn}{dE} &\sim \frac{4}{v} \frac{dJ}{dE} \\ &\sim 1.1 \times 10^{-4} E^{-2.2} \text{ electrons } (\text{cm}^3 \text{keV})^{-1}. \end{aligned} \quad (5)$$

If we assume that this density is representative of the average density over the cone, the total number of particles injected becomes

$$\frac{dN}{dE} \sim V \frac{dn}{dE} \sim 10^{36} E^{-2.2} \text{ electrons keV}^{-1}. \quad (6)$$

The total number of electrons above 20 keV is then $N(>20 \text{ keV}) \sim 2 \times 10^{34}$. Similar numbers are obtained from diffusion-theory calculations.

3. Analysis

A. FLARE LOCATION

The flare responsible for the phenomena studied here probably occurred in McMath active region 11953. This identification is consistent with the timing of the type II

and type III bursts, and with the NW limb location of the coronal optical and radio phenomena observed at Culgoora. Furthermore, the solar particle event had the characteristics expected of flares in the W 20–W 80 longitude range, implying that the flare in question could not have occurred far beyond the limb. Given this identification, the flare location was N 20, W 110 if it occurred at the same heliographic coordinates as a flare at McMath region 11953, 19 July, 1972, 05:40 UT. This location corresponds to an occultation height, the altitude of the tangent ray from the Earth, of $\sim 45\,000$ km. This small active region produced only a single confirmed subflare during its life on the solar disk. The occurrence of such an energetic event in such a feeble active region is remarkable, but strong circumstantial evidence supports this choice.

B. THE ENERGETIC PARTICLE POPULATION

The data described above give independent means for estimating the physical parameters in the emitting region. We assume initially that both the X-ray and radio emissions came from a common, uniform source located above the occultation height of $\sim 45\,000$ km.

The unusually low peak frequency of the microwave spectrum indicates that part of the source was occulted (Stewart and Nelson, 1979). As a preliminary estimate we can assume a density typical of the corona at the occultation height, namely $\sim 10^8$ cm $^{-3}$ (Newkirk, 1961), and a magnetic field of ~ 10 G (Dulk and McLean, 1978). This density and field strength are consistent with a Razin cutoff frequency $< 10^9$ Hz (Ramaty and Petrosian, 1972). The bremsstrahlung X-radiation and gyrosynchrotron microwave emission determine two non-overlapping parts of the instantaneous non-thermal electron spectrum in the source at maximum:

$$\begin{aligned} \frac{dN}{dE} &= 9.1 \times 10^{35} E^{-1.5}, & 20 < E < 200 \text{ keV} \\ &= 1.4 \times 10^{39} E^{-3}, & 3 < E < 10 \text{ MeV}, \end{aligned} \quad (7)$$

where for the latter we have used the formula in Tucker (1975) for the gyrosynchrotron emission. Extrapolating these two spectra toward each other gives a break at ~ 130 keV. Note the general similarity in slope and break energy of this spectrum and the spectra of escaping electrons in Figure 9, and X-rays in Figure 6. Although the low-energy electron spectrum at the Sun (i.e., that inferred from the X-rays) is flatter by 0.7 power in the steady state (after 03:47 UT) than the escaping electron spectrum, at the onset of the event at 03:44 UT the X-ray spectrum was significantly steeper than its steady value. Thus, at the X-ray event onset the X-ray producing electrons had essentially the *same* spectrum as the escaping electrons. An obvious interpretation is that at the X-ray burst onset we are observing freshly accelerated electrons and with time the continuing acceleration comes to an equilibrium with the loss processes. If the major loss process is Coulomb collisions the spectrum will tend to become flatter as observed. Based on the rate of spectral

hardening the observed time scale for such flattening was $\sim 10^2$ s. This is consistent with the collisional energy loss time for $E = 25$ keV and an assumed density $n_i = 10^8 \text{ cm}^{-3}$.

The observations then are consistent with a single acceleration mechanism which supplies both electrons which escape to the interplanetary medium and electrons which stay at the Sun. The electrons at the Sun lose energy predominantly via collisions, producing a flattening of the spectrum which continues until equilibrium is reached between the continuous acceleration and collision losses (at $\sim 03:47$ UT). Once the acceleration stops spectral flattening should start again. Since no significant flattening was observed up to $04:10$ UT we believe the acceleration continued to that time, at which point the X-ray emission was too low for analysis. If the type II shock wave was the accelerating agent, the fact that type II radio emission was observed up through $\sim 04:15$ UT is consistent with this interpretation.

We can quantitatively describe a simple homogeneous model for the X-ray source region by using the continuity equation:

$$\frac{\partial N(E, t)}{\partial t} = F(E, t) + \frac{N(E, t)}{\tau_e} - \frac{d}{dE} \left[N(E, t) \frac{dE}{dt} \right], \quad (8)$$

where $N(E, t)$ is the instantaneous electron spectrum in the source and $F(E, t)$ is the injection spectrum. The rightmost term describes particle energy variations and the next to last term on the right gives the loss of particles from the X-ray source region by 'escape'. The escape time τ_e could be a function of energy and/or time. We shall assume that Coulomb collisions constitute the only important energy change process. From Trubnikov (1966) the energy loss by collisions in ionized hydrogen is given by

$$\frac{dE}{dt} = -4.9 \times 10^{-9} n_i E^{-1/2} \text{ keV s}^{-1}. \quad (9)$$

No direct information is available on the loss term. The electrons may escape to a low density region where they no longer produce significant X-ray fluxes. We assume here that the electrons leave the X-ray source through a fixed exit area so that $\tau_e = l/v$ where l is a constant. Note that these electrons are not necessarily escaping to the interplanetary medium. Assuming that the X-ray source has an average density of $n_i = 10^8 \text{ cm}^{-3}$ we can obtain $N(E, t)$ from the observed X-ray spectra. We then solve Equation (8) to obtain $F(E, t)$ and adjust the constant of proportionality, l , for the electron loss term to obtain the same spectral shape for $F(E, t)$ as the observed spectrum in the interplanetary medium. Making the fit at the observed time for injection, we find $l \sim 10^{12} \text{ cm}$ for $n_i = 10^8 \text{ cm}^{-3}$. Using this value of l we then solve the equation numerically, energy channel by energy channel, to obtain the energy dependence of $F(E, t)$. The results are shown in Figure 10. Note that $F(E, t)$ has a relatively close fit to a power law at all times, and that the slope remains essentially constant over the event even though the intensity of F varies substantially. Integrating over the event we obtain the total accelerated

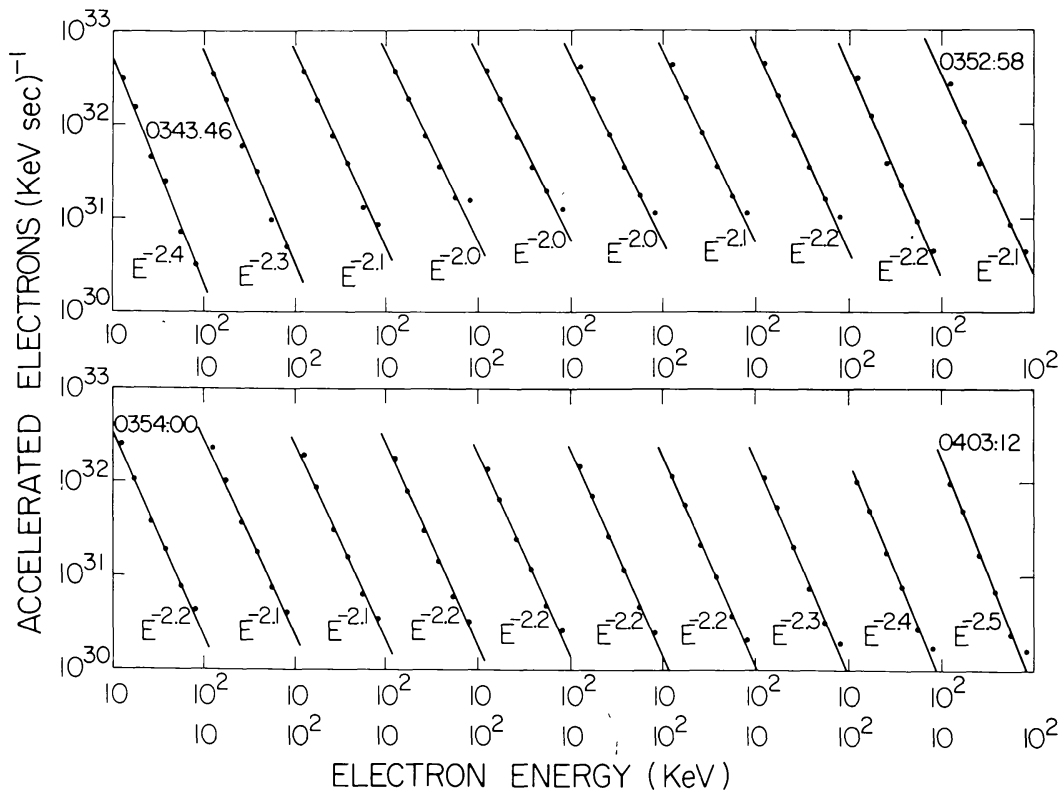


Fig. 10. Computed spectra of source electrons, as computed from the theory given in the text, compared with the distribution derived from the hard X-ray spectrum.

electron spectrum, the spectra of electrons lost by collisions and those lost by escape. These are shown in Figure 11 along with the interplanetary electron spectrum. Note that escape dominates collisional loss above ~ 45 keV but as expected collisions dominate at low energies. Of the total energy in the accelerated 20–100 keV electrons $\sim 50\%$ goes to collisions; the electrons escaping to the interplanetary medium are $\sim 1\%$ of the total accelerated. This ratio is larger than typical ($\sim 10^{-3}$) for impulsive events (Lin and Hudson, 1971, 1976); however the X-ray estimate is a lower limit (a) because any thin- or partially thin-target source produces X-radiation less efficiently, and (b) because the occultation geometry presumably excludes a large fraction of the X-ray source from the line of sight. The estimate for escaping electrons attempts to account for all of the particles, but is also very likely a lower limit because we have not taken into account longitudinal gradients which are likely to exist since the flare (W 110) is so far away in solar longitude from the W 60 connection longitude. There appears to be some suggestion, then, that the escape fraction in this second stage is larger than in impulsive events, but still small in absolute terms.

C. THE ACCELERATING AGENT

The observed time delays between the various radio, X-ray and particle phenomena provides strong evidence that the type II burst shock wave is the primary accelerating

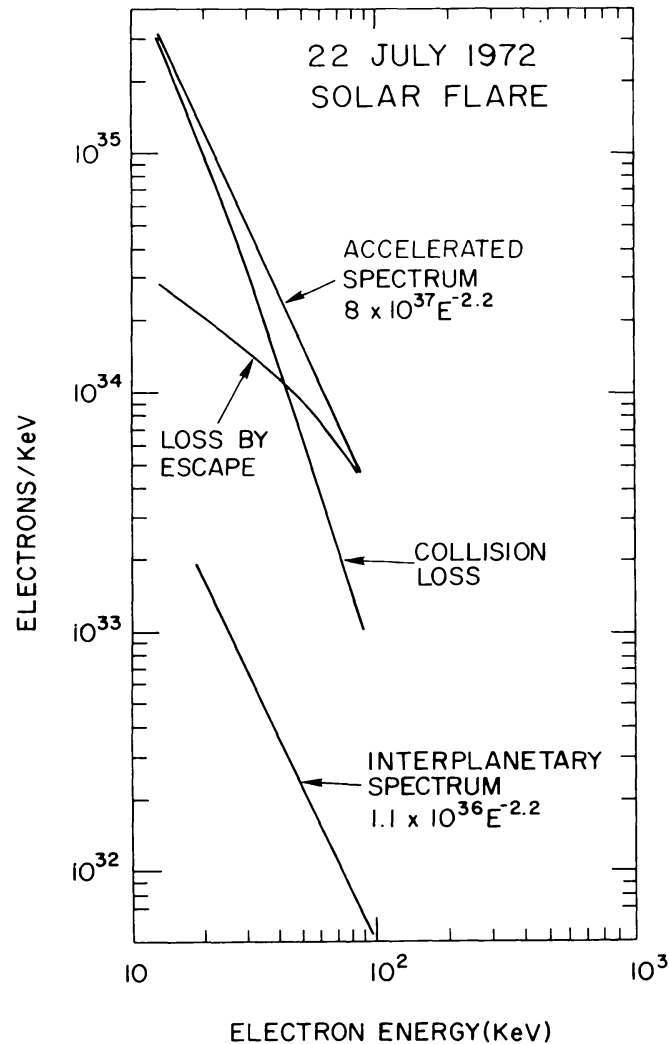


Fig. 11. Comparison of the computed electron distributions with the interplanetary observations. As described in the text, an injection spectrum $E^{-2.2}$ enables all of the observations to be reconciled with a simple theory in which the bulk of the electrons remain trapped near the Sun.

agent for the second stage. In particular the observed injection of electrons onto interplanetary field lines follows the impulsive phase by 22 min, exactly the time required for a shock front travelling at the inferred shock speed of 630 km s^{-1} to expand spherically outward from the flare at W 110 longitude and reach the field line at W 60, the connection longitude for the Earth. The timing of the FC II, the X-ray and microwave emission are all consistent with the hypothesis that the shock wave is the accelerating agent.

As indicated earlier (see Figure 3) the type II burst onset and drift rate are consistent with the shock originating at the flare itself during the impulsive phase. The type II emission itself is presumed to be produced by fast electrons accelerated at the shock. These electrons then produce plasma waves at the plasma frequency which in turn produce electromagnetic emission near the plasma frequency and twice the plasma frequency. This emission began at $\sim 03:40$ UT, about the time the shock reached the 80 MHz emission level.

D. THE FC II EMISSION MECHANISM

According to Dulk *et al.* (1978), a non-thermal particle density exceeding about one per Debye cell is a necessary condition for plasma radiation. The density of non-thermal particles in the FC II source may be estimated from its observed area. Using $V = A^{3/2}$, and taking the area of the FC II source at 80 MHz to be $4 \times 10^{21} \text{ cm}^2$, we find a volume of $2.5 \times 10^{32} \text{ cm}^3$. The non-thermal particle density (from Equation (2)) is therefore $n_{NT} \sim 2 \times 10^{11}/n_i$. For acceptable densities $n_{NT} \sim 10^3 \text{ cm}^{-3}$, whereas the volume of a Debye cell is about 1 cm^3 for $T = 3 \times 10^6 \text{ K}$, $n = 10^8 \text{ cm}^{-3}$. We therefore conclude that the plasma emission mechanism is feasible. The alternative, gyroresonance emission, is unlikely in a homogeneous model because of the low-frequency turnover at 1 GHz due to self-absorption (Stewart and Nelson, 1979). However, the generation of plasma waves also requires a positive-slope distribution function. We conclude that plasma-wave conversion is the probable origin of the FC II, within the limits of the present model.

4. Conclusions

The coronal effects of the behind-the-limb flare of 22 July 1972 extended throughout the electromagnetic and particle spectra. The various phenomena observed are probably related to local non-thermal particle acceleration produced by the passage of a large-scale shock wave through different structures: acceleration on closed field lines led to trapped particles responsible for meter-wave emission by plasma-wave conversion, microwave emission by the gyrosynchrotron process, and X-radiation by thick-target bremsstrahlung. Acceleration on open field lines released a very similar particle spectrum into interplanetary space, but with $\sim 1\%$ of the total particle number. The output spectrum of the accelerator was flat at low energies and steepened at higher energies, with the 'break' energy $\sim 130 \text{ keV}$. Since the acceleration took place in different locations with the same result, we conclude that the acceleration mechanism tends to be independent of some of the actual physical parameters in the medium.

Quantitative results have been obtained under the assumption of a homogeneous source for the different radiations. Such a source can consistently explain all of the phenomena, and we identify it with the tops of large loop structures extending above the occultation height of $\sim 45\,000 \text{ km}$.

The timing of the gradual X-ray event strongly implies that the particle acceleration observed occurred in a true second phase, delayed in time from the impulsive phase. The circumstance of limb occultation has enabled us to establish conclusively that the site of this second-stage acceleration is remote from the flare proper. The gamma-ray observations of major flares on the solar disk (Chupp *et al.*, 1973; Hudson *et al.*, 1980) and the 'extended X-ray bursts' (Hoyng *et al.*, 1976) represent other effects of the second-stage acceleration, which apparently works efficiently in the low corona near the location of the first-stage energy release.

Acknowledgments

Research in solar high-energy astrophysics at UCSD is supported by NASA under grant NSG-7161. The research at UCB is supported in part by NGL-05-003-017.

References

- Chupp, E. L., Forrest, D. J., Higbie, P. R., Suri, A. N., Tsai, C., and Dunphy, P. P.: 1973, *Nature* **241**, 333.
- Dulk, G. A. and McLean, D. J.: 1978, *Solar Phys.* **57**, 279.
- Dulk, G. A., Smerd, S. F., McQueen, R. M., Gosling, J. T., Magun, A., Stewart, R. T., Sheridan, K. V., Robinson, R. D., and Jacques, S.: 1976, *Solar Phys.* **49**, 369.
- Dulk, G. A., Melrose, D. B., and Smerd, S. F.: 1978, *Proc. Astron. Soc. Australia* **3**, 243.
- Elcan, M. J.: 1979, Ph.D. dissertation, University of California, San Diego.
- Gergely, T. E., Kundu, M. R., Munro, R. H., and Poland, A. I.: 1979, *Astrophys. J.* **230**, 575.
- Hoyng, P., Brown, J. C., and van Beek, H. F.: 1976, *Solar Phys.* **48**, 197.
- Hudson, H. S.: 1978, *Astrophys. J.* **224**, 235.
- Hudson, H. S., Bai, T., Gruber, D. E., Matteson, J. L., Nolan, P. L., and Peterson, L. E.: 1980, *Astrophys. J. Letters* **236**, L91.
- Lin, R. P.: 1974, *Space Sci. Rev.* **16**, 189.
- Lin, R. P. and Hudson, H. S.: 1971, *Solar Phys.* **17**, 412.
- Lin, R. P. and Hudson, H. S.: 1976, *Solar Phys.* **50**, 153.
- Lin, R. P., Mewaldt, R. A., and van Hollebeke, M. A. I.: 1981, submitted to *Astrophys. J.*
- Newkirk, G.: 1961, *Astrophys. J.* **133**, 983.
- Ramaty, R. and Petrosian, V.: 1972, *Astrophys. J.* **178**, 241.
- Robinson, R. D. and Smerd, S. F.: 1975, *Proc. Astron. Soc. Australia* **2**, 274.
- Stewart, R. T. and Nelson, G. J.: 1979, *Proc. Astron. Soc. Australia* **3**, 380.
- Stewart, R. T., Howard, R. A., Hansen, F., Gergely, T., and Kundu, M.: 1974a, *Solar Phys.* **36**, 203.
- Stewart, R. T., McCabe, M. K., Koomen, M. J., Hansen, R. T., and Dulk, G. A.: 1974b, *Solar Phys.* **36**, 219.
- Trubnikov, B. A.: 1966, *Rev. Plasma. Phys.* **1**, 105.
- Tucker, W. H.: 1975, *Radiation Processes in Astrophysics*, MIT, p. 125.
- van Hollebeke, M. A. I., MaSung, L. S., and McDonald, F. B.: 1975, *Solar Phys.* **41**, 189.
- Wild, J. P., Smerd, S. F., and Weiss, A. A.: 1963, *Ann. Rev. Astron. Astrophys.* **1**, 291.